

Quantum-enhanced sensing of photonic modes with cat states

Xiao-Wei Zheng¹, Jun-Cong Zheng¹, Xue-Feng Pan¹, and Pengbo Li^{1*}
¹*School of Physics, Xi'an Jiaotong University, Xi'an 710049, China*

(Dated: April 1, 2025)

Quantum coherence is critical resource for applications in quantum technology, among which quantum-enhanced sensing represents a typical example. Compared with quantum metrology with entangled states of multiple qubits, bosonic interferometers have the advantage of being hardware-efficient, enabled by exploiting the high-dimensional Hilbert space of a bosonic mode. Phase estimations with precisions approaching the Heisenberg limit have been demonstrated with superpositions of highly nonclassical Fock states of a single bosonic mode. We here present a scheme for realizing quantum metrology based on a fundamentally distinct kind of superposition states—Schrödinger cat states, defined as quantum superpositions of two quasiclassical (coherent) states of a bosonic mode. The interferometer aims to estimate the frequency shift of the photonic mode with respect to a reference frequency. The phase-space rotation due to such a frequency shift, together with a displacement operation, produces a phase difference between these two superposed quasiclassical state components, that can be extracted with a qubit. The signal-to-noise ratio exhibits a scaling approaching the Heisenberg limit, like interferometers based on Fock state superpositions, but without requiring a step-by-step procedure to prepare the resource state.

INTRODUCTION

The capability of building a high-sensitive interferometer for performing a high-precision measurement on physical quantity is crucial for advancement of science and technology [1-5]. In a standard interferometer, the physical quantity to be measured is encoded in a phase shift θ in one arm of the interferometer, and then estimated by interferometric techniques. The uncertainty of the phase estimation $\Delta\theta$ can arise from classical noises or quantum fluctuations. One strategy to mitigate the influence of noises is to prepare N identical interfering particles and average over all the measurement outcomes, with the precision scaling with N in a manner depending whether and how the particles are correlated. When these particles are not correlated or classical correlated, the phase uncertainty is reduced by a factor proportional to $1/\sqrt{N}$, as exemplified by a coherent state of a light field with N photons that exhibits no quantum effects. Such a standard quantum limit (SQL) can be surpassed when these N particles are prepared in nonclassically correlated states, among which the N -qubit Greenberger–Horne–Zeilinger (GHZ) state [6] is a paradigm, with which the precision exhibits a $1/N$ scaling, known as Heisenberg limit (HL) [5].

So far, entanglement-enhanced metrology has been demonstrated in a variety of platforms, including optical systems [7-12], Bose-Einstein Condensates [13-17], trapped ions [18-22], nuclear magnetic resonance [23], a superconducting circuit [24], and an atom array trapped in an optical lattice [25]. In principle, the sensitivity can be improved with the increase of the size of the entangled state, but which requires more hardware overhead, including the entangled elements and corre-

sponding readout apparatuses. Fortunately, entanglement is not the necessary resource for quantum-enhanced metrology [5,26]. Recently, superpositions of Rydberg states of single atoms were demonstrated to be useful for realizing high-sensitivity probes beyond SQL [27-29]. Bosonic modes represent an alternative promising candidate for implementation of quantum-enhanced metrology in a resource-efficient manner, enabled by their infinite dimensional Hilbert space. Single-mode interferometers have been built with a mechanical oscillator [30] and with a photonic field stored in a microwave cavity [31], where HL was approached by exploiting the quantum coherence between the ground state ($|0\rangle$) and a high-quantum-number Fock state ($|N\rangle$) of the bosonic mode. Quantum-enhanced metrology with Fock states has also been demonstrated [32,33]. Generally, preparation of such nonclassical probe states with a large N requires a step-by-step procedure [30] or a projective measurement, which converts a quasiclassical coherent state into the desired quantum state in a probabilistic manner [33,34].

Cat states of bosonic modes represent another kind of typical nonclassical states [35]. Such states are formed by coherent states with different amplitudes or phases. Although coherent states themselves are robust quasiclassical components, cat states can exhibit strong nonclassical features, as a consequence of the quantum interference effects between the quasiclassical components. The tunnelling probability between two superimposed quasiclassical components is exponentially suppressed with the increase of their distance in phase space [36,37]. This robustness makes cat states a promising candidate for construction of inherently-protected qubits for encoding quantum information [38-40]. Metrological power of such states has been theoretically analyzed from the viewpoint of quantum resources [41], and its application in the

high-precision detection of a phase-space displacement has been investigated in both theory [42,43] and experiment [44,45]. The authors of Ref. [43] also proposed a protocol for quantum-enhanced measurement of rotations of a bosonic mode, where an entangled mesoscopic state involving the bosonic mode and a qubit serves as the quantum resource. After the rotation, the qubit-field entanglement is undone by their interaction, but the field evolution trajectories associated with the two qubit states accumulate a phase difference, which can be measured by measuring the qubit's population. The sensitivity scales with the phase-space separation between the two photonic coherent states of the initial mesoscopic entanglement. As the field's rotation is produced by the deviation of the frequency of the photonic field from a reference frequency, the field frequency can be inferred from the rotation angle. The protocol is valid only when the phase uncertainty of the qubit is negligible during the field's rotation. However, in real physical systems (e.g., circuit QED architectures [46]), the dephasing time of the qubit may be much shorter than that of the photonic mode. As a consequence, the quantum advantage may be deteriorated by the phase noise of the qubit accumulated during the field's rotation.

We here present an alternative protocol for estimating the frequency shift of a photonic mode with the superposition of an amplitude cat state, formed by the vacuum state and a coherent state. Such a frequency shift can result in a rotation of the coherent state in phase space. This signal can be encoded to the state of a qubit by performing a phase-space displacement on the photonic mode, and then sandwiching a qubit-state-dependent π -phase shift of the photonic mode between two $\pi/2$ pulses applied to the qubit. In distinct contrast with the protocol of Ref. [43], the photonic mode is not entangled with the qubit during the rotation, so that the purity of the superposition state is not deteriorated by the qubit dephasing during this stage. The numerical results show that the precision of phase estimation is improved with the increase of the cat size, with the scaling approaching the HL. We further show that this protocol can be adapted to the estimation of the frequency of mechanical oscillators. The most remarkable feature of this metrological method is that the preparation of a cat state is much more easy than that of the Fock state or its superposition with the vacuum state with the same size. It can be created deterministically with a procedure where the number of steps does not increase with the cat size [46].

THE PROTOCOL

Let us begin by illustrating how a coherent state $|\alpha_0\rangle$ can be used to amplifying the rotation produced by a

frequency shift of a bosonic mode. In the framework rotating at a reference frequency ω_0 , the system evolution is governed by the free Hamiltonian

$$H = \varepsilon a^\dagger a, \quad (1)$$

where ε represents the frequency shift with respect to a reference frequency, and a^\dagger and a denote the creation and annihilation operators for the bosonic mode. This frequency shift results in a phase-space rotation, evolving the coherent state $|\alpha_0\rangle$ to $|\alpha_0 e^{i\theta}\rangle$, where $\theta = -\varepsilon T$ with T being the evolution time. The quantum-mechanical phase difference between this rotated coherent state and the original one is defined as the argument of the inner product is $\phi = \arg \langle \alpha_0 | \alpha_0 e^{i\theta} \rangle = D \sin \theta$, where $D = |\alpha_0|^2$ is mean quantum number of the coherent state $|\alpha_0\rangle$. When $\theta \ll 1$, $\phi \simeq D\theta$. This implies that the quantum-mechanical phase accumulated during the time T is proportional to D .

To detect this frequency-shift-induced phase, it is necessary to prepare the bosonic mode in the cat state

$$\mathcal{N}(|0\rangle + |\alpha_0\rangle), \quad (2)$$

where $|0\rangle$ denotes the vacuum component which serves as a reference state and does not evolve under the phase-space rotation, and $\mathcal{N} = (1 + e^{-D/2})^{-1/2}/\sqrt{2}$ is the normalization factor. As the two superimposed quasi-classical state components differ from each other by the amplitude, the superposition state is referred to as an amplitude cat state. Under the application of the Hamiltonian of Eq. (1) for a time T , this state evolves to $\mathcal{N}(|0\rangle + |\alpha_0 e^{i\theta}\rangle)$. Since any coherent state has a zero phase difference relative to the vacuum component, a phase-space displacement operation $D(-\alpha_0/2)$ is needed to produce an observable phase difference. This displacement respectively transforms $|0\rangle$ and $|\alpha_0 e^{i\theta}\rangle$ to $|\alpha_0/2\rangle$ and $e^{iD\theta/2} |\alpha_0'/2\rangle$, where $\alpha_0' = \alpha_0(2e^{i\theta} - 1)$. Consequently, the cat state is evolved to

$$\mathcal{N}(|-\alpha_0/2\rangle + e^{iD\theta/2} |\alpha_0'/2\rangle). \quad (3)$$

When $\theta \ll 1$, the two coherent states approximately have the same amplitude, and differ from each other by their phases. The resulting superposition state is referred to as the phase cat state. The corresponding phase difference can be detected by the Ramsey interferometry, realized by sandwiching a conditional π -phase shift $G_\pi = (-1)^{a^\dagger a} |e\rangle \langle e|$ between two $\pi/2$ qubit rotation, $e^{-i\pi\sigma_y/4}$, where $\sigma_y = i|e\rangle \langle g| - i|g\rangle \langle e|$ with $|e\rangle$ and $|g\rangle$ denoting the qubit's upper and lower levels, respectively. The conditional π -phase shift G_π is realized by dispersively coupling the bosonic mode to the qubit [46]. The dispersive interaction is described by the Hamiltonian $H_I = -\chi a^\dagger a |e\rangle \langle e|$, where χ denotes the dispersive coupling strength between the qubit and the bosonic mode.

With the choice of the interaction time π/χ , the dispersive interaction results in π -phase shift to the qubit's state $|e\rangle$ conditional on the parity of the quantum number of the bosonic mode being odd.

The qubit and the bosonic mode is evolved to an entangled state at the output of the Ramsey interferometer, given by

$$\frac{\mathcal{N}}{\sqrt{2}} [(|-\alpha_0/2\rangle + e^{iD\theta/2} |\alpha'_0/2\rangle) |\psi_+\rangle + (|\alpha_0/2\rangle + e^{iD\theta/2} |-\alpha'_0/2\rangle) |\psi_-\rangle], \quad (4)$$

where

$$|\psi_{\pm}\rangle = (|e\rangle - |g\rangle) / \sqrt{2}. \quad (5)$$

This result shows that the Ramsey interferometer splits each of the two input quasiclassical component into two components with opposite phases. The resulting quantum interference leads to the θ -dependence of the qubit's $|g\rangle$ -state population,

$$P_g = \mathcal{N}^2 \{ 1 - (e^{-D/2} + e^{-D'/2})/2 + e^{-(D+D')/8} \text{Re}[e^{iD\theta/2}(e^{-\alpha_0^* \alpha'_0/4} - e^{\alpha_0^* \alpha'_0/4})] \} \quad (6)$$

where $D' = |\alpha'_0|^2$. Fig. 1a shows this probability as a function of D and θ . As expected, when D is sufficiently large and θ is sufficiently small, P_g approximately exhibits an oscillatory pattern, whose period decreases as D increases. This is due to the fact that P_g can be well approximated by $\mathcal{C}(\theta) = [1 - \cos(D\theta)]/2$ when $D \gg 1$ and $D\theta^2/2 \ll 1$. To show this behavior more clearly, we display P_g as a function of θ for $D = 50$ in Fig. 1b, which confirms the ultra-sensitive response of P_g to slight change of θ during the regime $0 < \theta < \pi/(2D)$.

The performance of the sensor is characterized by the signal-to-noise ratio, defined by

$$R = \frac{|\partial P_g / \partial \theta|}{\sqrt{P_g(1 - P_g)}}. \quad (7)$$

The interferometer aims to estimate the deviation of θ from a bias point θ_0 . To make the interferometer be able to distinguish the sign of deviation, we set $D\theta_0 = \pi/2$. At such a bias point, the signal-to-noise ratio can be approximated by $R \simeq D$. This implies that the interference presents an approximately linearly improved sensitivity with the increase of the mean photon number, approaching the HL when the decoherence is negligible. We note that a similar scaling has been demonstrated with the Fock-state superposition, $(|0\rangle + |N\rangle)/\sqrt{2}$ [30,31]. However, the pulse sequence for preparing such a superposition and for recombining the two Fock-state components becomes more complex with the increase of N . In distinct contrast, the number of steps for preparing and manipulating the cat state is generally independent of the

size of the cat state [46]. To confirm the validity of the approximation, we perform a numerical simulation of R . Fig. 1c presents R as a function of D at the bias point

$\theta_0 = \pi/(2D)$. The result shows that the signal-to-noise ratio almost linearly scales with the size of the cat state.

EFFECT OF DECOHERENCE

The main problem for the implementation of the our protocol is the photonic dissipation of the cat state. We suppose that the time needed to prepare the cat state and that to read out the signal are much shorter than the time needed to accumulate the phase θ , so that the decoherence during the cat state preparation and the dispersive coupling can be neglected. With the decoherence effect during the free evolution of the cat state being taken into consideration, the system combined by the photonic mode and qubit finally evolves to the mixed state, described by the density operator

$$\frac{\mathcal{N}^2}{2} [\rho_p \otimes |\psi_+\rangle \langle \psi_+| + \Pi \rho \Pi \otimes |\psi_-\rangle \langle \psi_-| + \Pi \rho \otimes |\psi_-\rangle \langle \psi_+| + \rho \Pi \otimes |\psi_+\rangle \langle \psi_-|]. \quad (8)$$

where $|\psi_{\pm}\rangle$ are given by Eq. (5), $\Pi = e^{-i\pi a^\dagger a}$, and

$$\rho_p = \mathcal{N}^2 (|-\alpha_0/2\rangle \langle -\alpha_0/2| + |\alpha''_0/2\rangle \langle \alpha''_0/2| + (K e^{-i\phi} |-\alpha_0/2\rangle \langle \alpha''_0/2| + H.c.)), \quad (9)$$

with $K = e^{-|\alpha_0|^2(1-e^{-\kappa T})/2}$, $\phi = \frac{1}{2} |\alpha_0|^2 e^{-\kappa T/2} \sin \theta$, and $\alpha''_0 = \alpha_0(2e^{i\theta - \kappa T/2} - 1)$, with κ being the photonic decaying rate. The probability of detecting the qubit in the state $|g\rangle$ is

$$P_g = \mathcal{N}^2 \{ 1 - (e^{-D/2} + e^{-D''/2})/2 + K e^{-(D+D'')/8} \text{Re}[e^{i\phi}(e^{-\alpha''_0 \alpha_0^*/4} - e^{\alpha''_0 \alpha_0^*/4})] \} \quad (10)$$

where $D'' = |\alpha''_0|^2$.

Fig. 2a displays this probability as a function of θ and κT with the choice $D = 50$. As expected, when κT and θ are sufficiently small, P_g also approximately exhibits an oscillatory pattern, but with a reduced contrast compared to the case without considering decoherence. The result can be well understood by considering the conditions $D \gg 1$, $D\theta^2/2 \ll 1$, and $\kappa T \ll 1$, under which P_g can be well approximated by $P_g = [1 - e^{-|\alpha_0|^2 \kappa T/2} \cos(D\theta)]/2$. Fig. 2b presents the signal-to-noise ratio R versus D and κT at the bias point $\theta_0 = \pi/(2D)$. Due to the presence of decoherence, R does not show the linear scaling. There is a tradeoff between the gain from the enhanced sensitivity of the total phase $D\theta$ and the reduced contrast of the interference fringe.

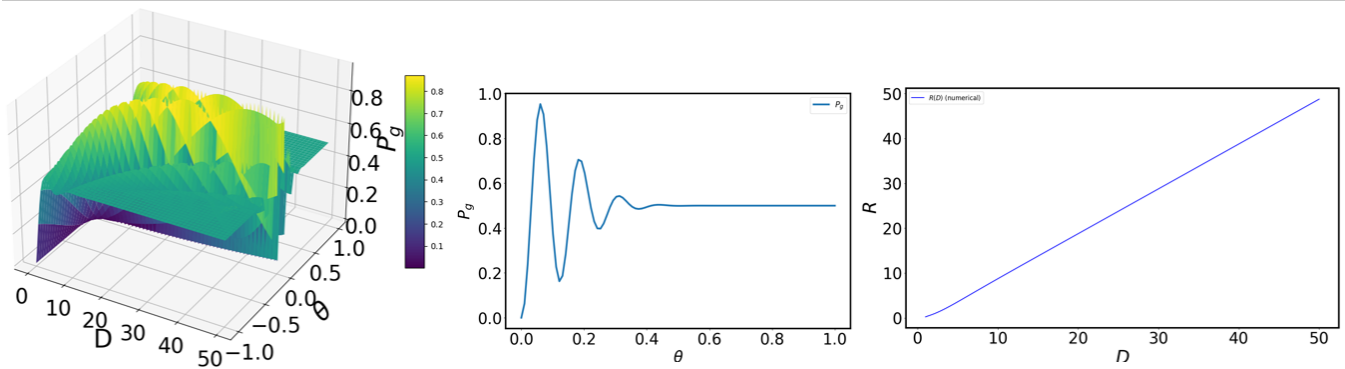


FIG. 1. Quantum sensing without decoherence. (a) The qubit's $|g\rangle$ -state population (P_g) as a function of D and θ . (b) P_g as a function of θ for $D = 50$. (c) Signal-to-noise ratio (R) as a function of D at the bias point $\theta_0 = \pi/(2D)$.

To illustrate this point more clearly, in Fig. 2c we present R as a function of D with the choice $\kappa T = 0.02$. As expected, R does not monotonously increase with D . It reaches the maximum of 36.25 at the point $D = 100$, and then decreases due to the linearly increasing decoherence rate of the cat state.

CONCLUSION

In conclusion, we have proposed a scheme for realizing a quantum-enhanced interferometer based on an amplitude cat state, formed by the vacuum state and a coherent state of a photonic mode. The frequency shift of the bosonic mode with respect to a reference frequency leads to a phase-space rotation of the coherent state. The rotation angle can be estimated by the Ramsey interference of a qubit dispersively coupled to the bosonic mode, following a displacement operation, transforming the amplitude cat state into a phase cat state. The Ramsey interferometry involves two $\pi/2$ pulses, in between which a qubit-state-dependent π -phase shift of the bosonic mode is sandwiched. The output qubit's ground state population depends upon the rotation angle of the bosonic mode, with the sensitivity of being proportional to the size of the cat state. Our results opens a promising prospect for quantum metrology in a resource-efficient manner.

This work was supported by the National Natural Science Foundation of China under Grant No..

Fig. 1 (color online). Quantum sensing without decoherence. (a) The qubit's $|g\rangle$ -state population (P_g) as a function of D and θ . (b) P_g as a function of θ for $D = 50$. (c) Signal-to-noise ratio (R) as a function of D at the bias point $\theta_0 = \pi/(2D)$.

point $\theta_0 = \pi/(2D)$.

Fig. 2 (color online). Quantum sensing with decoherence. (a) The qubit's $|g\rangle$ -state population as a function

of θ and κT for $D = 50$. (b) Signal-to-noise ratio R versus D and κT . (c) R versus D for $\kappa T = 0.02$. In both (b) and (c), R is calculated at the bias point $\theta_0 = \pi/(2D)$.

-
- [1] R. X. Adhikari, Gravitational radiation detection with laser interferometry, *Rev. Mod. Phys.* 86, 121 (2014).
 - [2] V. Giovannetti, S. Lloyd, and L. Maccone, Quantum-enhanced measurements: Beating the standard quantum limit, *Science* 306, 1330 (2004).
 - [3] C. L. Degen, F. Reinhard, and P. Cappellaro, Quantum sensing, *Rev. Mod. Phys.* 89, 035002 (2017).
 - [4] L. Pezzè, A. Smerzi, M. K. Oberthaler, R. Schmied, and P. Treutlein, Quantum metrology with nonclassical states of atomic ensembles, *Rev. Mod. Phys.* 90, 035005 (2018).
 - [5] D. Braun, G. Adesso, F. Benatti, R. Floreanini, U. Marzolino, M. W. Mitchell, and S. Pirandola, Quantum-enhanced measurements without entanglement. *Rev. Mod. Phys.* 90, 035006 (2018).
 - [6] D. M. Greenberger, M. A. Horne, and A. Zeilinger, *Bell's Theorem, Quantum Theory and Conceptions of the Universe* (Springer, 1989).
 - [7] T. Nagata, R. Okamoto, J. L. O'Brien, K. Sasaki, and S. Takeuchi, Beating the standard quantum limit with four entangled photons, *Science* 316, 726 (2007).
 - [8] R. Krischek, C. Schwemmer, W. Wieczorek, H. Weinfurter, P. Hyllus, L. Pezzè, and A. Smerzi, Useful multi-particle entanglement and sub-shot-noise sensitivity in experimental phase estimation, *Phys. Rev. Lett.* 107, 080504 (2011).
 - [9] S. Slussarenko, M. M. Weston, H. M. Chrzanowski, L. K. Shalm, V. B. Verma, S. W. Nam, and G. J. Pryde, Unconditional violation of the shot-noise limit in photonic quantum metrology, *Nat. Photonics* 11, 700 (2017).
 - [10] L.-Z. Liu, Y.-Z. Zhang, Z.-D. Li, R. Zhang, X.-F. Yin, Y.-Y. Fei, L. Li, N.-L. Liu, F. Xu, Y.-A. Chen, and J.-W. Pan, Distributed quantum phase estimation with entangled photons, *Nat. Photonics* 15, 137 (2021).
 - [11] C. F. Ockeloen, R. Schmied, M. F. Riedel, and P. Treutlein, Quantum metrology with a scanning probe atom interferometer, *Phys. Rev. Lett.* 111, 143001 (2013).

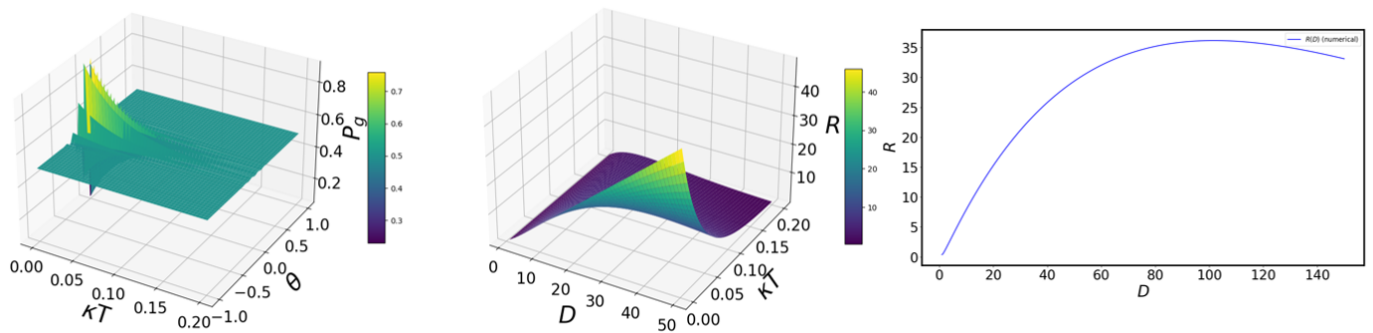


FIG. 2. Quantum sensing with decoherence. (a) The qubit's $|g\rangle$ -state population as a function of θ and κT for $D = 50$. (b) Signal-to-noise ratio R versus D and κT . (c) R versus D for $\kappa T = 0.02$. In both (b) and (c), R is calculated at the bias point $\theta_0 = \pi/(2D)$.

- [12] C. Zhang, T. R. Bromley, Y.-F. Huang, H. Cao, W.-M. Lv, B.-H. Liu, C.-F. Li, G.-C. Guo, M. Cianciaruso, and G. Adesso, Demonstrating quantum coherence and metrology that is resilient to transversal noise, *Phys. Rev. Lett.* 123, 180504 (2019).
- [13] W. Muessel, H. Strobel, D. Linnemann, D. B. Hume, and M. K. Oberthaler, Scalable spin squeezing for quantum-enhanced magnetometry with Bose-Einstein condensates, *Phys. Rev. Lett.* 113, 103004 (2014).
- [14] O. Hosten, N. J. Engelsen, R. Krishnakumar, and M. A. Kasevich, Measurement noise 100 times lower than the quantum-projection limit using entangled atoms, *Nature (London)* 529, 505 (2016).
- [15] S. Colombo, E. Pedrozo-Penafiel, A. F. Adiyatullin, Z. Li, E. Mendez, C. Shu, and V. Vuletić, Time-reversal-based quantum metrology with many-body entangled states, *Nature Physics* (2022).
- [16] Q. Liu, L.-N. Wu, J.-H. Cao, T.-W. Mao, X.-W. Li, S.-F. Guo, M. K. Tey, and L. You, Nonlinear interferometry beyond classical limit enabled by cyclic dynamics, *Nature Physics* 18, 167 (2022).
- [17] G. P. Greve, C. Luo, B. Wu, and J. K. Thompson, Entanglement-enhanced matter-wave interferometry in a high-finesse cavity, *Nature (London)* 610, 472 (2022).
- [18] D. Leibfried, M. D. Barrett, T. Schaetz, J. Britton, J. Chiaverini, W. M. Itano, J. D. Jost, C. Langer, and D. J. Wineland, Toward Heisenberg-limited spectroscopy with multiparticle entangled states, *Science* 304, 1476 (2004).
- [19] D. Leibfried, E. Knill, S. Seidelin, J. Britton, R. B. Blakestad, J. Chiaverini, D. B. Hume, W. M. Itano, J. D. Jost, C. Langer, R. Ozeri, R. Reichle, and D. J. Wineland, Creation of a six-atom “Schrödinger cat” state, *Nature (London)* 438, 639 (2005).
- [20] T. Monz, P. Schindler, J. T. Barreiro, M. Chwalla, D. Nigg, W. A. Coish, M. Harlander, W. Hänsel, M. Hennrich, and R. Blatt, 14-qubit entanglement: Creation and coherence,” *Phys. Rev. Lett.* 106, 130506 (2011).
- [21] J. G. Bohnet, B. C. Sawyer, J. W. Britton, M. L. Wall, A. M. Rey, M. Foss-Feig, and J. J. Bollinger, Quantum spin dynamics and entanglement generation with hundreds of trapped ions, *Science* 352, 1297 (2016).
- [22] L. Pezzè, Y. Li, W. Li, and A. Smerzi, Witnessing entanglement without entanglement witness operators, *PNAS* 113, 11459 (2016).
- [23] X. Long, W.-T. He, N.-N. Zhang, K. Tang, Z. Lin, H. Liu, X. Nie, G. Feng, J. Li, T. Xin, Q. Ai, and D. Lu, Entanglement-enhanced quantum metrology in colored noise by quantum Zeno effect, *Phys. Rev. Lett.* 129, 070502 (2022).
- [24] K. Xu, Y.-R. Zhang, Z.-H. Sun., H. Li, P. Song, Z. Xiang, K. Huang, H. Li, Y.-H. Shi, C.-T. Chen, X. Song, D. Zheng, F. Nori, H. Wang, and H. Fan, Metrological characterization of non-Gaussian entangled states of superconducting qubits, *Phys. Rev. Lett.* 128, 150501 (2022).
- [25] A. Cao, W. J. Eckner, T. L. Yelin, A. W. Young, S. Jandura, L. Yan, K. Kim, G. Pupillo, J. Ye, N. D. O’pong, and A. M. Kaufman, Multi-qubit gates and Schrödinger cat states in an optical clock, *Nature (London)* 634, 315 (2024).
- [26] B. L. Higgins, D. W. Berry, S. D. Bartlett, H. M. Wiseman, and G. J. Pryde, Entanglement-free Heisenberg-limited phase estimation, *Nature (London)* 450, 393-396 (2007).
- [27] A. Facon, E.-K. Dietsche, D. Grosso, S. Haroche, J.-M. Raimond, M. Brune, and S. Gleyzes, A sensitive electrometer based on a Rydberg atom in a Schrödinger-cat state, *Nature (London)* 535, 262 (2016).
- [28] E. K. Dietsche, A. Larrouy, S. Haroche, J. M. Raimond, M. Brune, and S. Gleyzes, High-sensitivity magnetometry with a single atom in a superposition of two circular Rydberg states, *Nat. Phys.* 15, 326 (2019).
- [29] T. Chalopin, C. Bouazza, A. Evrard, V. Makhlov, D. Dreon, J. Dalibard, L. A. Sidorenkov, and S. Nascimbene, Quantum-enhanced sensing using non-classical spin states of a highly magnetic atom, *Nat. Commun.* 9, 4955 (2018).
- [30] K. C. McCormick, J. Keller, S. C. Burd, D. J. Wineland, A. C. Wilson, and D. Leibfried, Quantum-enhanced sensing of a mechanical oscillator, *Nature* 572, 86 (2019).
- [31] W. Wang, Y. Wu, Y. Ma, W. Cai, L. Hu, X. Mu, Y. Xu, Zi-Jie Chen, H. Wang, Y. P. Song, H. Yuan, C.-L. Zou, L.-M. Duan, and L. Sun, Heisenberg limited single-mode quantum metrology, *Nature Communications* 10, 4382 (2019).
- [32] F. Wolf et al., Motional Fock states for quantum-enhanced amplitude and phase measurements with trapped ions, *Nat. Commun.* 10, 2929 (2019).
- [33] X. Deng, S. Li, Z.-J. Chen, Z. Ni, Y. Cai, J. Mai, L. Zhang, P. Zheng, H. Yu, C.-L. Zou, S. Liu, F. Yan, Y. Xu, and D. Yu, Quantum-enhanced

- metrology with large Fock states, *Nat. Phys.* (2024). <https://doi.org/10.1038/s41567-024-02619-5>.
- [34] W. Wang, L. Hu, Y. Xu, K. Liu, Y. Ma, S.-B. Zheng, R. Vijay, Y. P. Song, L.-M. Duan, and L. Sun, Converting quasiclassical states into arbitrary Fock state superpositions in a superconducting circuit, *Phys. Rev. Lett.* 118, 223604 (2017).
- [35] V. Bužek, A. Vidiella-Barranco, and P. L. Knight, Superpositions of coherent states: Squeezing and dissipation, *Phys. Rev. A* 45, 6570 (1992).
- [36] R. Lescanne, M. Villiers, T. Peronin, A. Sarlette, M. Delbecq, B. Huard, T. Kontos, M. Mirrahimi, and Z. Leghtas, Exponential suppression of bit-flips in a qubit encoded in an oscillator, *Nature Physics* 16, 509 (2020).
- [37] A. Grimm, N. E. Frattini, S. Puri, S. O. Mundhada, S. Touzard, M. Mirrahimi, S. M. Girvin, S. Shankar, and M. H. Devoret, Stabilization and operation of a kerr-cat qubit, *Nature* 584, 205 (2020).
- [38] J. Guillaud and M. Mirrahimi, Repetition cat qubits for fault-tolerant quantum computation, *Phys. Rev. X* 9, 041053 (2019).
- [39] S. Puri, L. St-Jean, J. A. Gross, A. Grimm, N. E. Frattini, P. S. Iyer, A. Krishna, S. Touzard, L. Jiang, A. Blais, S. T. Flammia, and S. M. Girvin, Bias-preserving gates with stabilized cat qubits, *Sci. Adv.* 6, eaay5901 (2020).
- [40] N. Ofek, A. Petrenko, R. Heeres, P. Reinhold, Z. Leghtas, B. Vlastakis, Y. Liu, L. Frunzio, S. M. Girvin, L. Jiang, M. Mirrahimi, M. H. Devoret, and R. J. Schoelkopf, Extending the lifetime of a quantum bit with error correction in superconducting circuits, *Nature* 536, 441 (2016).
- [41] H. Kwon, K. C. Tan, T. Volkoff, and H. Jeong, Nonclassicality as a quantifiable resource for quantum metrology, *Phys. Rev. Lett.* 122, 040503 (2019).
- [42] W. J. Munro, K. Nemoto, G. J. Milburn, S. L. Braunstein, Weak-force detection with superposed coherent states, *Physical Review A* 66, 023819 (2002).
- [43] F. Toscano, D. A. R. Dalvit, L. Davidovich, and W. H. Zurek, Sub-planck phase-space structures and heisenberg-limited measurements, *Phys. Rev. A* 73, 023803 (2006).
- [44] C. Hempel, B. P. Lanyon, P. Jurcevic, R. Gerritsma, R. Blatt, and C. F. Roos, Entanglement-enhanced detection of single-photon scattering events, *Nat. Photonics* 7, 630 (2013).
- [45] M. Penasa, S. Gerlich, T. Rybarczyk, V. Métillon, M. Brune, J. M. Raimond, S. Haroche, L. Davidovich, and I. Dotsenko, Measurement of a microwave field amplitude beyond the standard quantum limit, *Phys. Rev. A* 94, 022313 (2016).
- [46] B. Vlastakis, G. Kirchmair, Z. Leghtas, S. E. Nigg, L. Frunzio, S. M. Girvin, M. Mirrahimi, M. H. Devoret, R. J. Schoelkopf, Deterministically encoding quantum information using 100-photon Schrödinger cat states. *Science* 342, 607–610 (2013).